Electronic Supplementary Material (ESI) for Nanoscale Advances.

Supporting Information

Revealing the alloying and dealloying behaviors in AuAg nanorods by thermal stimulus

Long-Bing He,*[a, b], Lei Shangguan,[a] Ya-Ting Ran,[a] Chao Zhu,[a] Zi-Yu Lu,[a] Jiong-Hao Zhu,[a] Dao-Jiang Yu ,[a] Cai-Xia Kan,*[c] Li-Tao Sun,[a, b]

[a]SEU-FEI Nano-Pico Center, Key Laboratory of MEMS of Ministry of Education, Southeast University, Nanjing 210096, P. R. China.
Emails: helongbing@seu.edu.cn

[b]Centre for Advanced Materials and Manufacture, Joint Research Institute of Southeast University and Monash University, Suzhou 215123, P. R. China.

[c]College of Physics, Nanjing University of Aeronautics and Astronautics, No. 29 Jiangjun Road, Nanjing 211106, P. R. China.
Emails: cxkan@nuaa.edu.cn

1. Morphology of the as-synthesized AuAg nanorods

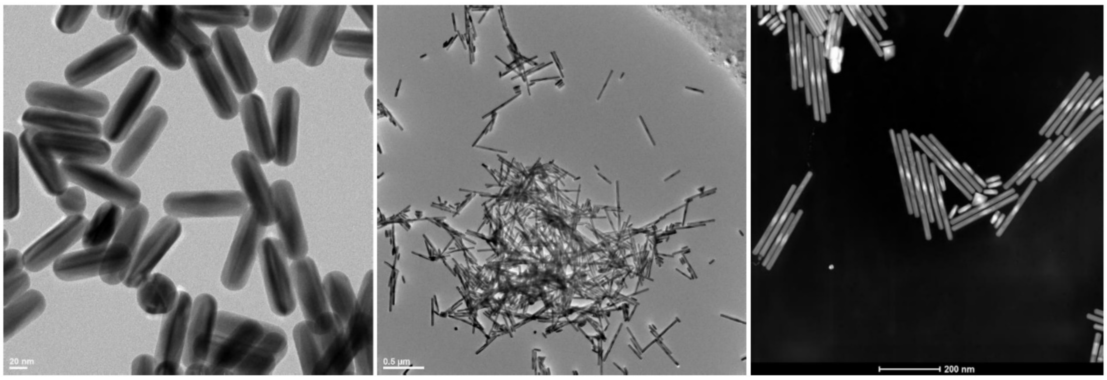

Figure S1. Morphology of the as-synthesized AuAg nanorods. The lengths of the nanorods can be designed by controlling the growth process over the Au seeds.

2. Heterointerfaces in the as-synthesized AuAg nanorods

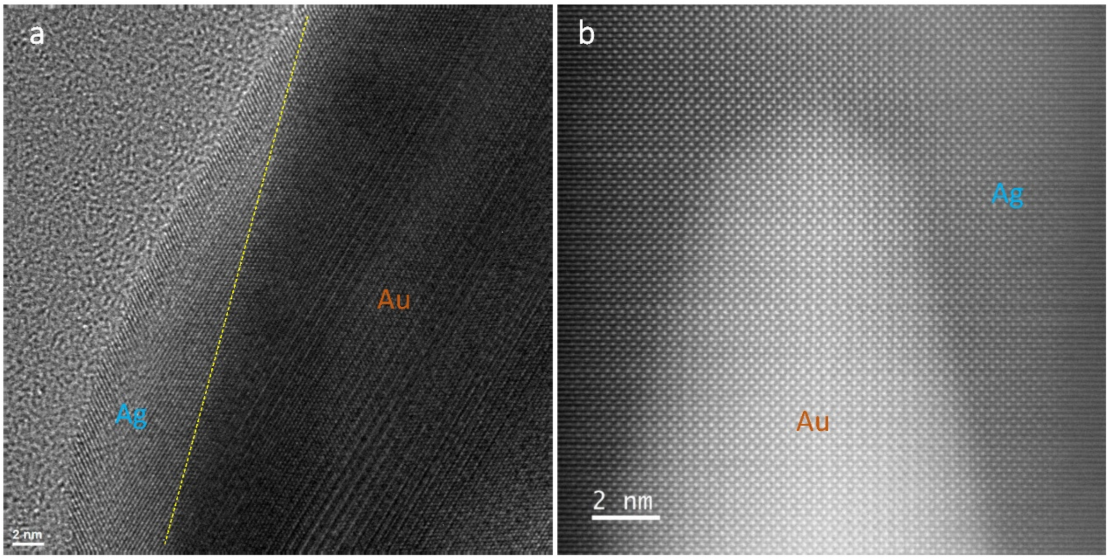

Figure S2. (**a**) High-resolution TEM image of a heterointerface of a short AuAg nanorod. (**b**) Atomistic STEM image of a heterointerface of a long AuAg nanorod.

3. Interdiffusion-induced alloying in the AuAg nanorods

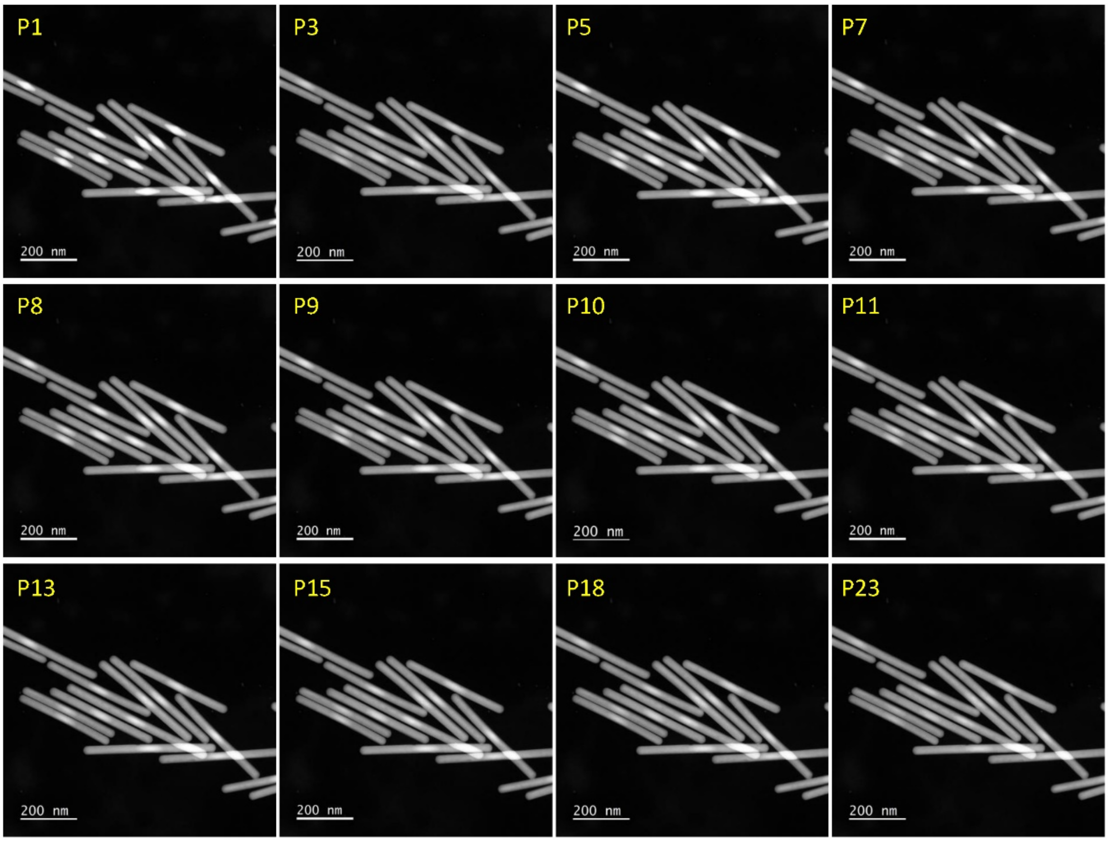

Figure S3. Dark-field STEM images showing the evolution of a bundle of AuAg nanorods under different thermal pulses. The thermal pulse is set to be 450 °C with a duration time of 1 s. P1 to P23 indicate the number of thermal pulses that have been exerted.

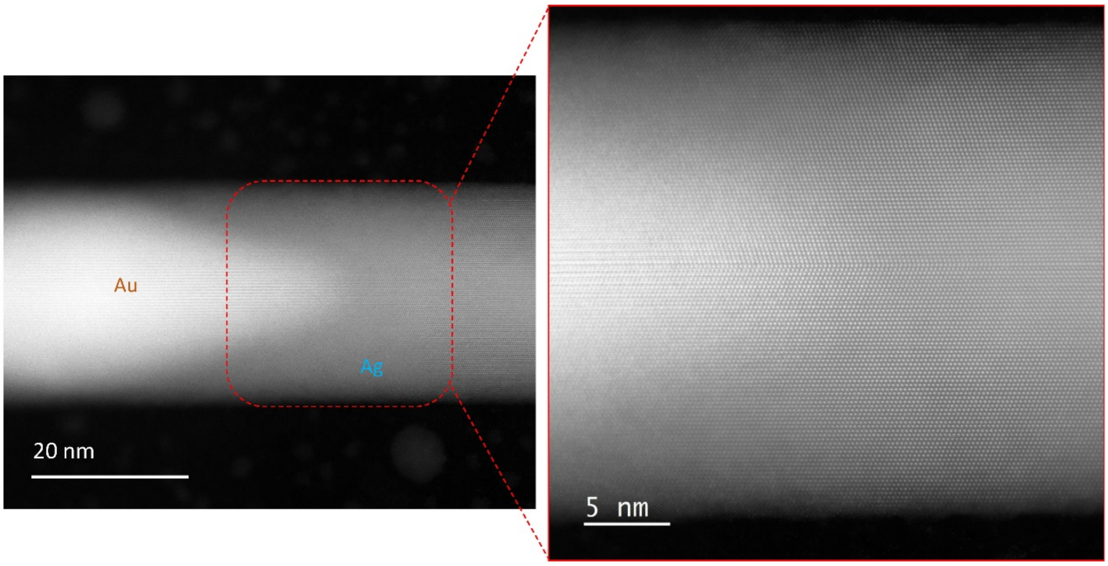

Figure S4. Atomic-resolution STEM images showing the evolution of the Au-Ag interfacial region under one thermal pulse of 350 °C for 1 s. The initial sharp interface turns to be blurry, though the Au core can still be identified accurately.

4. EDS mapping of the Au-Ag interface during alloying

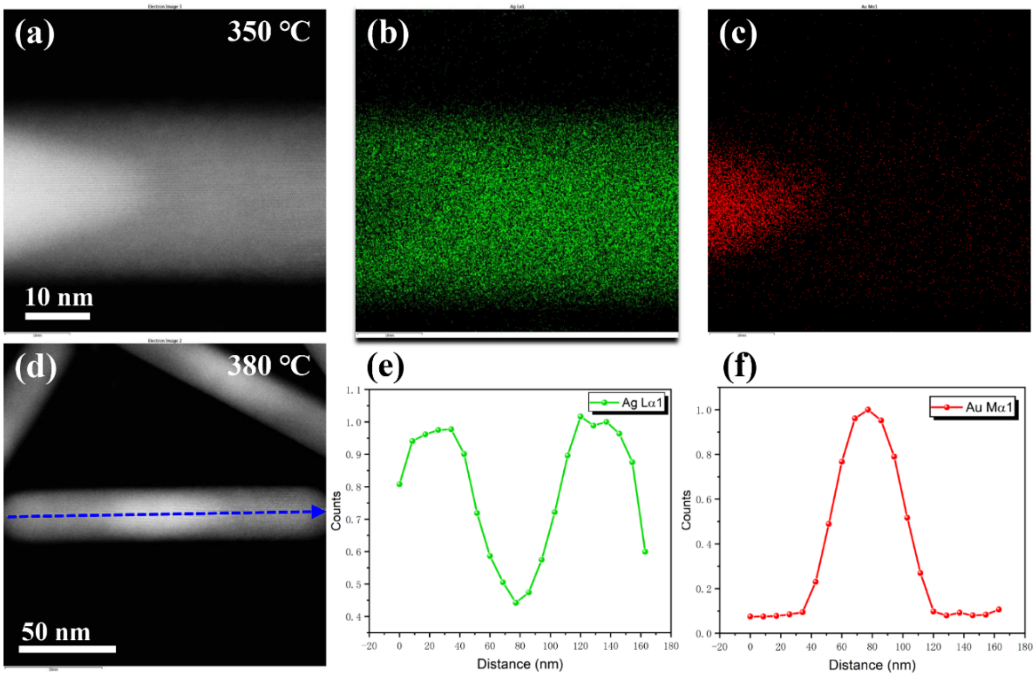

Figure S5. (**a**) High-resolution STEM image of a AuAg nanorod after it is treated with five thermal pulses. The thermal pulse is set as 350 °C for 1 s. (**b-c**) EDS mappings of the diminutions of Ag and Au, respectively. (**d**) STEM image of another AuAg nanorod that has been treated with six thermal pulses. The thermal pulse is set as 380 °C for 1 s. (**e-f**) Corresponding EDS line profiles of Ag and Au, respectively, as marked in (d).

5. Vapor pressures of Au and Ag as a function of temperature

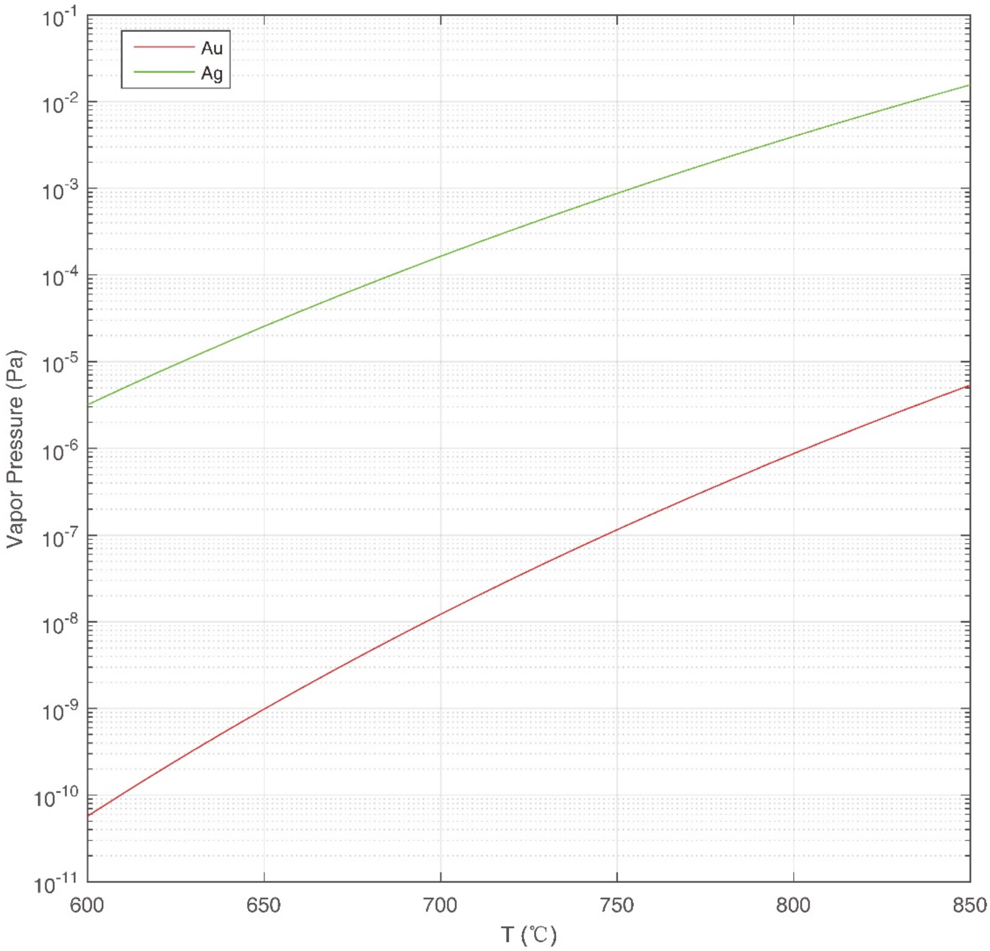

Figure S6. Vapor pressure as a function of temperature for Au and Ag, respectively.

6. Illustration of thermal-stimulated alloying and de-alloying processes in AuAg nanorods

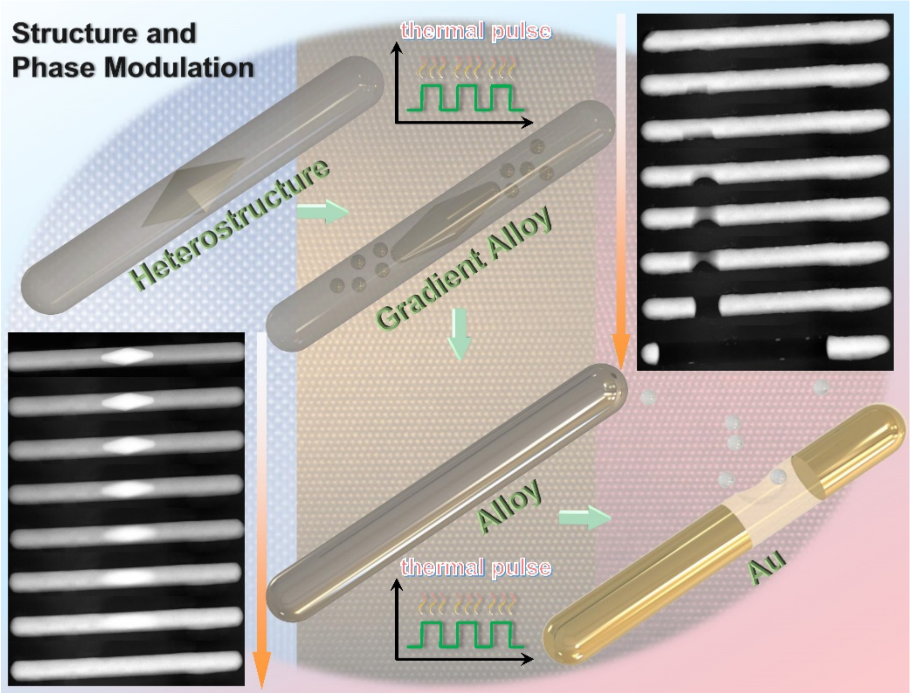

Figure S7. Schematic illustration of the structure and phase evolution of AuAg nanorods under thermal-pulse stimuli.

7. The formation of carbon shells on the AuAg nanorods

The formation of carbon shells on the AuAg nanorods is due to the decomposition of residual hydrocarbon molecules under the irradiation of electron beam. Hydrocarbon molecules and electron beam irradiation are two prerequisites, and carbon shells will not form without any of them. The growth of carbon shells can be controlled by controlling these two factors. For example, if the AuAg nanorods are washed many times, the residual surfactant molecules are rare and the formation of carbon shells is then difficult. Alternatively, the AuAg nanorod samples (dispersed on holey carbon grids) can be stored in a high-vacuum pump station for a whole night to desorb the volatile surfactant molecules so as to mitigate/avoid the growth of carbon shells during TEM imaging. In contrast, if one wants to form carbon shells on the AuAg nanorods, the hydrocarbon molecules are selectively remained. In this case, electron beam irradiation is a key parameter to control the carbon shell thickness. A low/moderate beam intensity is positive for carbon formation while an intense beam will lead to significant sputtering and sculpting of the carbon structure. By adjusting the beam intensity and irradiation time, the thickness of the carbon shells can be well controlled (Small 2014, 10, No. 9, 1724–1728).